



Biosynthesis of Nickel oxide Nanoparticles from *Euphorbia heterophylla* (L.) and their biological application

K. Lingaraju^a, H. Raja Naika^{a,*}, H. Nagabhushana^b, K. Jayanna^c, S. Devaraja^c, G. Nagaraju^d

^a Department of Studies and Research in Biotechnology, Tumkur University, Tumakuru 572103, India

^b Prof. C.N.R. Rao Centre for Advanced Material Science, Tumkur University, Tumakuru 572103, India

^c Department of Studies and Research in Biochemistry, Tumkur University, Tumakuru 572103, India

^d Department of Chemistry, Siddaganga Institute of Technology, Tumakuru 572103, India

Received 25 June 2019; accepted 12 November 2019

Available online 21 November 2019

KEYWORDS

Biosynthesis;
NiO NPs;
Characterization;
Biological applications

Abstract Nickel oxide Nanoparticles (NiO NPs) were synthesized from *E. heterophylla* (L.) leaves extract act as reducing/capping agent by biosynthesis process. Further the synthesized NiO NPs was subjected for structural, optical and biological properties. The XRD pattern of NiO NPS exhibit face centred cubic (FCC) crystalline structure. The UV-DR spectrum of biosynthesized NiO NPs exhibited optical properties with well-defined at 321 nm and its exhibits optical band gap is 3.24 eV. The FT-IR spectrum of NiO NPs shows stretching vibration of Ni-O at 452 cm⁻¹. The morphological features of NiO NPs are rhombohedra and slightly agglomerated and then size of the biosynthesized NiO NPs as found in the range of 12–15 nm. The NiO NPs shows vital non-toxic properties on human erythrocytes and its interference in activity coagulation cascade both on PRP and PPP on human blood. The Bactericidal activity of NiO NPs was shows significant inhibitory activity against pathogenic bacterial strains. Further, NiO NPs show significant cytotoxicity against human lung cancer cell line (A549) and human hepatocarcinoma (HepG2) cell lines. Therefore, the study reveals states that, the *E. heterophylla* (L.) leaves extract is an effective reducing/capping agent for the formation of NiO NPs and its exhibits biological properties.

© 2019 The Authors. Published by Elsevier B.V. on behalf of King Saud University. This is an open access article under the CC BY-NC-ND license (<http://creativecommons.org/licenses/by-nc-nd/4.0/>).

* Corresponding author.

E-mail address: rajanaiika@tumkuruniversity.ac.in (H. Raja Naika).

Peer review under responsibility of King Saud University.



Production and hosting by Elsevier

1. Introduction

In current years, among metal oxide nanoparticles have great attracted increasing attention due to the presence of different applications with highly remarkable with large surface area, band gap stability and reusability (Kaviyarasu et al., 2016; Sun et al., 2012; Hisatomi et al., 2014; Nandy et al., 2013;

Pereira et al., 2014; Hoffmann et al., 1995; Ezhilarasi et al., 2018) Nickel oxide Nanoparticles (NiO NPs) has fascinated greater attention due to their different flexible properties (Singh et al., 2016; Jahromi et al., 2015). Different methods have been used to synthesize of Nickel oxide Nanoparticles (NiO NPs) such as the sol-gel, solvothermal, hydrothermal, thermal decomposition, precipitation (Sankar et al., 2016; Qing et al., 2015; Motevalli et al., 2016; Nassar et al., 2017; Gnanasekaran et al., 2017). Most of these methods are highly expensive, tedious protocol, highly sophisticated instruments, toxic, non-eco-friendly for synthesis of Nanoparticles (Mohammadijoo et al., 2014). To overcome the problem of toxic wastes and energy imbalance, biocompatibility, greener and ecofriendly process for the synthesis of nanoparticles been suggested (Madhumitha et al., 2016). Towards, the biocompatibility synthesis of NiO NPs from plants such as *Moringa oleifera* (Ezhilarasi et al., 2016), *Tamarix serotina* (Nasseri et al., 2016) *Callistemon viminalis* (Sone et al., 2016), *Aegle marmelos* (Ezhilarasi et al., 2018) and *Agathosma betulina* (Thema et al., 2016) contains different bioactive chemicals with various functional groups its exhibiting different applications (Roopan and Khan, 2011; Manivel et al., 2009). During the biocompatible metal oxide nanoparticles metabolites play a crucial role in converting metal into metal nano form by reduction mechanism (Zhi-Guo et al., 2011).

In the present study, a complete biocompatibility assisted synthesis of Nickel oxide Nanoparticles has been reported by using the aqueous leaves extract of medicinal plant *Euphorbia heterophylla* (Linn.). *Euphorbia heterophylla* (Linn.) belongs to the Euphorbiaceae family. The medicinal value of *E. heterophylla* is well documented and it is mostly used in the treatment of various disorders (Falodun and Agbakwuru, 2004; Uduak et al., 2010; Keerthana et al., 2014; Falodun et al., 2006; Meenakshi Sundaram et al., 2010). Biosynthesis of Nickel oxide Nanoparticles (NiO NPs) has been successfully demonstrated in recent years and therefore there is a growing interest in NiO nanoparticles synthesis via biosynthesis process. Further, the bio synthesized NiO NPs was confirmed by using various techniques such as XRD, UV-DRS, FT-IR, SEM-EDX and TEM techniques. Furthermore, the biosynthesized Nickel oxide Nanoparticles (NiO NPs) from *E. heterophylla* (L.) was investigated by various biological properties including such as direct haemolytic and Anticoagulant properties, antibacterial and cytotoxicity.

2. Experimental

2.1. Chemicals

All the chemicals were purchased from Sigma Aldrich, SD-Fine and Himedia Laboratory Pvt. Ltd., India with analytical grade without further purification. All the aqueous solutions were prepared by using double distilled water throughout the experiments.

2.2. Preparation of extract and synthesis of NiO NPs

The preparation of extract from *E. heterophylla* (L.) leaves in aqueous medium by soxhlet extraction apparatus (Raja Naika and Krishna, 2006). In a typical experiment, 10 mL of aqueous leaves extract of *E. heterophylla* (1 mg/mL) and

90 mL of Nickel Nitrate hexahydrate ($\text{Ni}(\text{NO}_3)_2 \cdot 6\text{H}_2\text{O}$) (0.1 mM) were taken in a round bottomed flask. The mixture was then stirred vigorously with the help of magnetic stirrer at room temperature for 24 h. After stirring, the mixture was kept in dark condition to observe the colour and then bottom of the flask precipitate was formed. Then after, to collect the precipitate from bottom of the flask with the help of centrifuge at 10000 rpm for 30 min. After centrifugation, the clear supernatant was discarding and collects the pellet. The obtained pellet is again suspended in de-ionized distilled water and washed with several times to remove impurities for 2–3 times. Then after washing, the pellet was dried and calcined at 300 °C for 3 h. After calcination process, the product was crushed in to fine powder using mortar and pestle and then finally greyish black coloured product was obtained and kept it air tight container for further analysis.

2.3. Characterization

The phase purity and crystallinity of the biosynthesized NiO NPs was subjected to X-ray diffraction employing Shimadzu Powder X-ray diffractometer (PXRD) ($\text{CuK}\alpha$, $\lambda = 1.54 \text{ \AA}$) radiation with nickel filter. The Ultra Violet Diffuse reflectance spectrum was recorded using Perkin Elmer Lambda-35 Spectrophotometer. The functional groups analysis of biosynthesized NiO NPs was using Perkin Elmer Spectrum BXFT-IR system. The morphological features of biosynthesized NiO NPs was studied by scanning electron microscopy (SEM, Hitachi – 3000), EDAX analysis (Nova Nano SEM 600, FEI Company) and transmission electron microscopy (TEM) (Jeol tem3010) fitted with a Gatan CCD camera operating at an accelerating voltage of 300 kV.

2.4. Direct haemolytic and Anticoagulant properties

2.4.1. Direct haemolytic activity

The direct haemolytic activity of NiO NPs (40, 60, 80 and 100 μg) was determined by using human erythrocytes (Chethana et al., 2017). The haemolytic activity was expressed as percentage of haemolysis against percentage of lysis of cells due to presence of water (positive control) and phosphate buffered saline (negative control).

2.4.2. Anticoagulant activity

2.4.2.1. Preparation of platelet-rich plasma and platelet-poor plasma. The preparation of human platelet-rich plasma (PRP) and Platelet-poor plasma (PPP) was followed method (Ardlie and Han, 1974). The platelet concentration of PRP was adjusted to 3.1×10^8 platelets/ml with PPP. Above content was maintained at 37 °C for 2 h due to the process of blood coagulation. All the above preparations were carried out using plastic wares or silicon zed glass wares.

2.4.2.2. Plasma recalcification time. The plasma recalcification time was determined was followed by Quick et al., method (Quick et al., 1935). In a briefly, the various concentration of biosynthesized NiO NPs (0–100 μg) was pre-incubated with 0.2 mL of citrated human plasma in the presence of 10 mM Tris HCl (20 μl) buffer pH 7.4 for 1 min at 37 °C. Then after, the addition of 20 μl of 0.25 M CaCl_2 was pre incubated mixture and clotting time was recorded.

2.5. Antibacterial activity studies

The antibacterial activity of biosynthesized NiO NPs against pathogenic bacterial strains both Gram +ve *Staphylococcus aureus* (NCIM-5022) and Gram -ve bacteria *Escherichia coli* [NCIM-5051], *Pseudomonas desmolyticum* [NCIM-2028] and *Klebsiella aerogenes* [NCIM-2098] strains (Purchased from NCL Pune, India) by Agar well diffusion method (Manjunath et al., 2014). Nutrient agar plates were prepared by using 37.0 g of Nutrient agar media was dissolved in 1000 mL of distilled water, and then subject to the sterilized by autoclaved at (121 °C) 15 lbs pressure for 15–20 min. After sterilization, NA medium was poured into sterile petri-dishes and allowed to solidify then after, 100 µl of 24 h mature broth culture of individual pathogenic bacterial strains in nutrient broth while spreading all over the surface of agar plates using sterilized L-shaped glass rod. Thereafter, using the sterile steel cork borer 06 mm wells were made into the each petriplate under aseptic condition. Then after, different concentration of NiO NPs (200,400 and 600 µg/well) was dispersed in 10% DMSO solution and while standard antibiotic Ciprofloxacin used as a positive control and control in to the wells. The plates were incubated at 37 °C for 24 h. After the incubation period, to observe the Zone of inhibition around the wells was measured by using geometrical Vernier callipers in mm. The antibacterial bacterial activity was carried out in triplicate and then determining the bactericidal activity of NiO NPs.

2.6. Cytotoxicity of NiO NPs

The cytotoxicity of biosynthesized NiO NPs against human Lung cancer (A549) and Human Hepatocarcinoma (HepG2) cell line (National Centre for Cell Science, Pune, India) (Dhaneswar et al., 2013; Lingaraju et al., 2019; Ibraheem et al., 2019). The growing of cell lines in the presence of following Dulbecco's Modified Eagle's Medium (DMEM) with supplemented fetal bovine serum with antibiotics maintained at 37 °C in a humidified atmosphere of 5% CO₂ for 24 h. The cells were seeded in 96 well plates at a density 25 × 10³ cells/well. In the presence of MTT assay, the cytotoxicity of different concentration of biosynthesized NiO NPs (25, 50, 100, 200 and 400 µg/mL) against human cancer cell lines. MTT is a dye (Yellow in colour) which is reduced in to purple colour formazon crystals in the presence of activity shows in mitochondrial succinate dehydrogenase enzyme in viable cells. The statistical analysis of cytotoxicity of biosynthesized NiO NPs against cancer cell lines in the presence of MTT to viability of cell was evaluated the IC₅₀ value was determined.

3. Results and discussion

3.1. Characterization

The PXRD pattern of biosynthesized NiO NPs from *E. heterophylla* as shown in Fig. 1. All the peaks at 37.24, 43.29, 62.85, 75.38, 79.37 assign to the planes were indexed with (1 1 1), (2 0 0), (2 2 0), (3 1 1) and (2 2 2) respectively well matched with JCPDS Card no.04-0835 with FCC (Face centered cubic) crystalline Bunsenite structure of NiO NPs. No impurities were observed which suggests the high purity of monophasic NiO

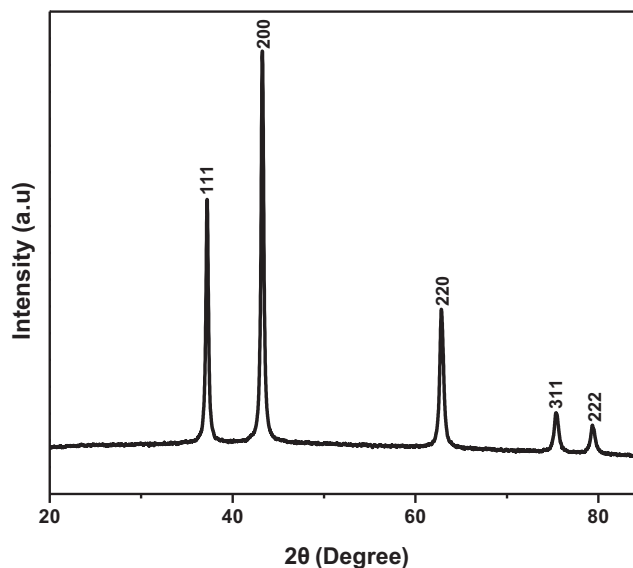


Fig. 1 Show the PXRD pattern of biosynthesis of NiO NPs.

nanoparticles. The average crystallite size of NiO NPs is found to be 15 nm in size was calculated using the Debye–Scherrer formula (Suresh et al., 2015).

$$D = \frac{k\lambda}{\beta \cos\theta} \quad (1)$$

where 'D' crystallite size of the 'k' shape factor (0.9), 'λ' wavelength of X-ray (1.54 Å) Cu Kα radiation, 'θ' is the Bragg angle from 2θ value of intensity peak from XRD pattern and 'β' is the FWHM of the diffraction of NiO NPs.

The UV-DR Spectrum of spectrum of biosynthesized NiO NPs was recorded between 300 and 800 nm as shown in Fig. 2. The UV-DR spectrum of NiO NPs at 321 nm (Fig. 2a) is due to the charge transfer from conduction band to valance band cations. The spectrum exhibits the toward shorter wavelength signals decrease in size of the particle.

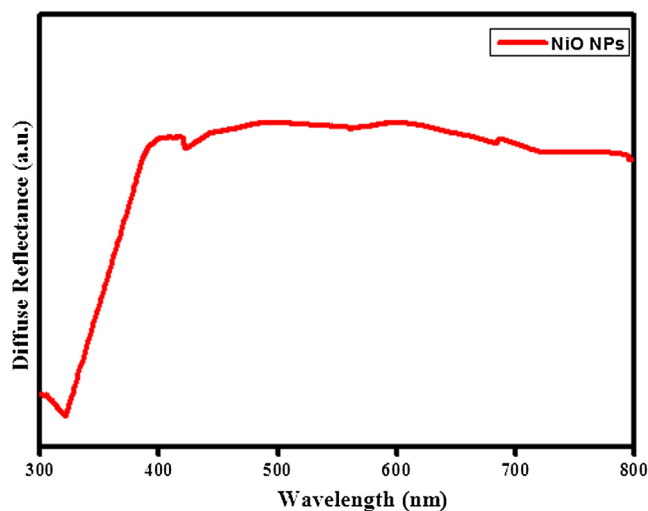


Fig. 2a UV-Diffuse reflectance spectrum of biosynthesis of NiO NPs.

As a result, assigned that the formation of oxides between the bond formations with functional groups to induced metal nucleation. The optical energy band gap (E_g) of the nanoparticles is estimated by Kubelka–Munk relation (K. Linga raju et al., 2019). The estimation of optical energy band gap (E_g) of biosynthesized NiO NPs is 3.24 eV as shown in the Fig. 2b.

The FTIR spectrum of biosynthesized NiO NPs from *E. heterophylla* as shown in the Fig. 3. The broad absorption peak at 3440 cm^{-1} belongs to O-H stretching vibrations indicates hydroxyl group which is generally phenolics and carboxylic acids. Another peak located at 1631 cm^{-1} is attributed to the bending mode (H-O-H) of water molecules. The characteristic absorption peaks of oxide groups belongs to 1037 cm^{-1} , 1112 cm^{-1} , 1388 cm^{-1} , 1462 cm^{-1} respectively. The other

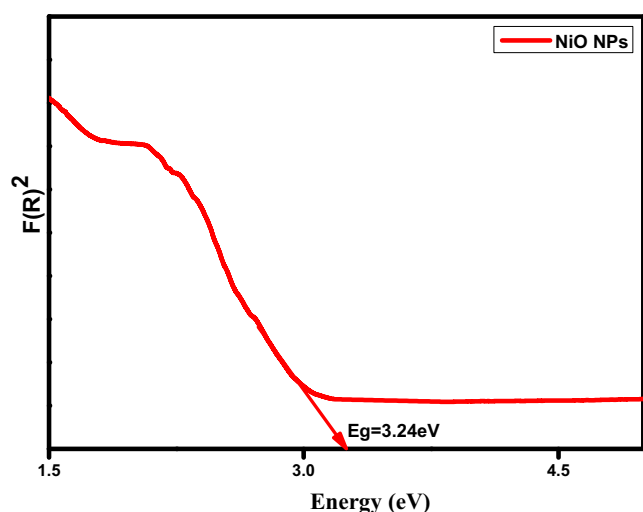


Fig. 2b Show the direct energy band gap (E_g) of biosynthesis of NiO NPs.

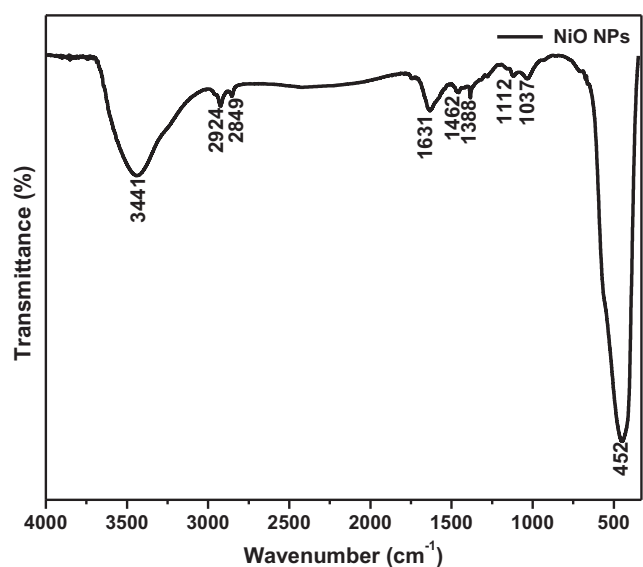


Fig. 3 Show the FT-IR spectrum of biosynthesized NiO NPs.

characteristics peak 2924 and 2849 cm^{-1} indicates the presence of OH group. The obtained peak at 452 cm^{-1} is caused by the Ni-O vibration. Thus, it is clearly indicating that, the phytochemicals take part in the biotransformation of nitrates to oxides. The phytochemicals from plant materials act as reducing agent during the formation of nanoparticles (Rajesh Kumar et al., 2013).

The morphological studies of biosynthesis of NiO NPs from leaves extract of *E. heterophylla* as shown in Fig. 4. The SEM micrograph of NiO NPs are rhombohedral in shapes and its agglomeration with particles on the surface area as show in the Fig. 4(a). However, TEM images of NiO NPs with an average particles size around $12\text{--}15\text{ nm}$ as in Fig. 4(b). The particle size determined from the particle size distribution diagram was very similar to the value of 15 nm obtained based on XRD data using Scherrer's formula. The element analysis of NiO NPs such as Ni and O varies periodically along with percentage of atom and weight as shown in the Fig. 4(c), there is no evidence of impurity in the composition. The morphological analysis of NiO NPs showed the effect of plant extract of *E. heterophylla*.

3.2. Biological properties

3.2.1. Direct haemolytic and Anticoagulant properties

3.2.1.1. Direct haemolytic activity. The direct haemolytic activity of biosynthesized NiO NPs on human RBC blood cells as shown in the Fig. 5. As a result, shows that the different concentration of biosynthesized NiO NPs did not hydrolyse on RBC while comparing the positive control (water) and negative control (PBS) on Human erythrocytes.

3.2.1.2. Anticoagulant activity. The identified the probable role of biosynthesized NiO NPs in coagulation cascade, plasma recalcification time was performed using both human platelet rich plasma (PRP) and platelet poor plasma (PPP) as shown in the Fig. 6. The significance of biosynthesized NiO NPs exhibited anticoagulant effects by enhancing the clotting time of both PRP and PPP from control 200 s to 350 s and 210 s to 379 s respectively. The different concentration of biosynthesized NiO NPs shows the maximum concentration consumed in both the cases was found to be $100\text{ }\mu\text{g/mL}$ and remain unchanged up on increased dose to $90\text{--}100\text{ }\mu\text{g/mL}$.

3.2.2. Antibacterial activity

The antibacterial activity of biosynthesized NiO NPs was screened against pathogenic bacterial strains Gram +ve *Staphylococcus aureus* and Gram -ve *Escherichia coli* *Pseudomonas desmolyticum* and *Klebsiella aerogenes* by agar well diffusion method. The inhibitory effect of biosynthesized NiO NP with different concentrations (200 , 400 and $600\text{ }\mu\text{g}/\mu\text{L}$) with respective positive control (Ciprofloxacin) and control as shown in Fig. 7. The result of antibacterial activity of NiO NPs shows higher significant in *E. coli* and moderate in *S. aureus*, *P. desmolyticum* and *K. aerogenes* as shown in the Table 1. The exact mechanism of bactericidal activity of NPs is not reported yet, but assumption for the studies, the nanoparticles were interact with bacterial cell effects change in morphology of cell membrane and their increasing the permeability, the interrupts the regular transport through plasma membrane and then finally cell was

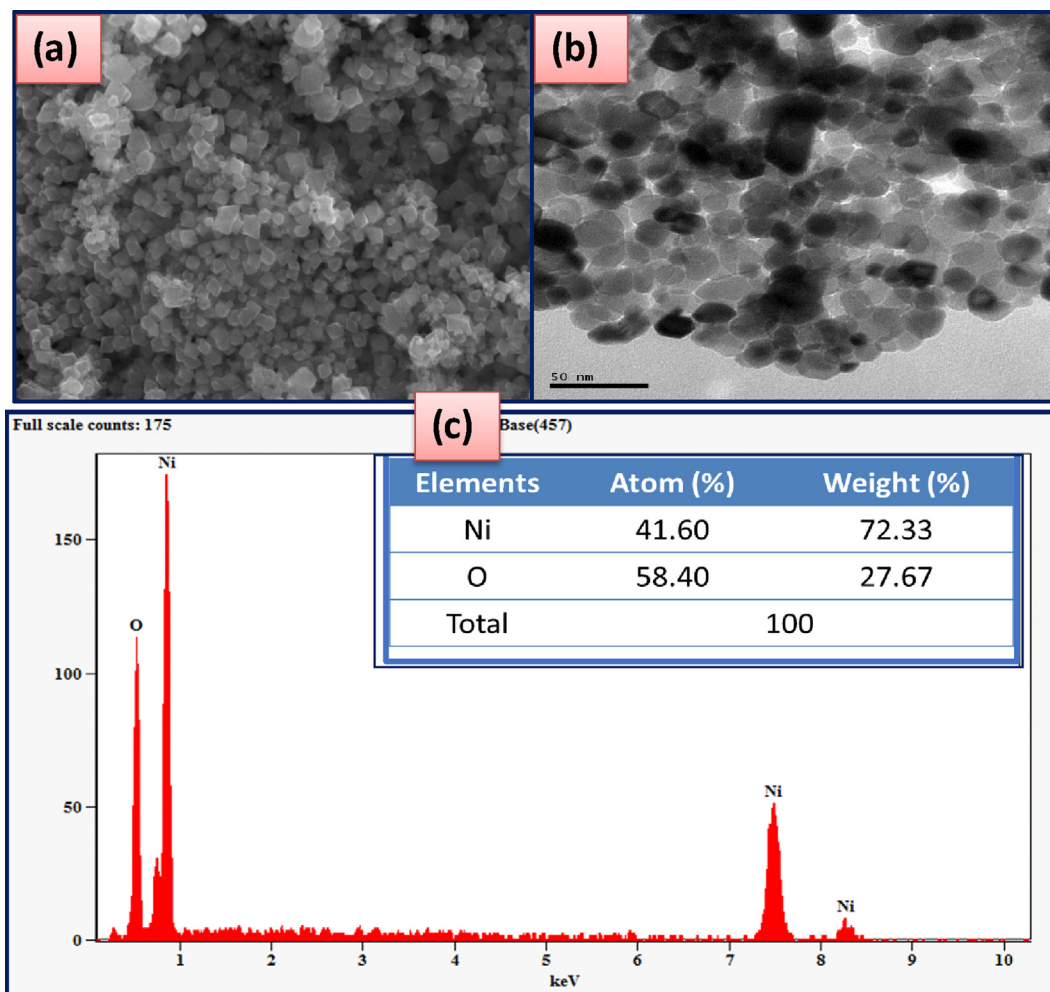


Fig. 4 Show the morphological features of biosynthesized NiO NPs (a) SEM micrograph (b) TEM images (c) EDAX.

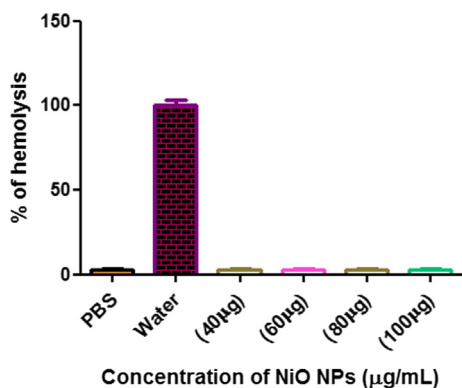


Fig. 5 Show the direct hemolytic activity of biosynthesized NiO NPs.

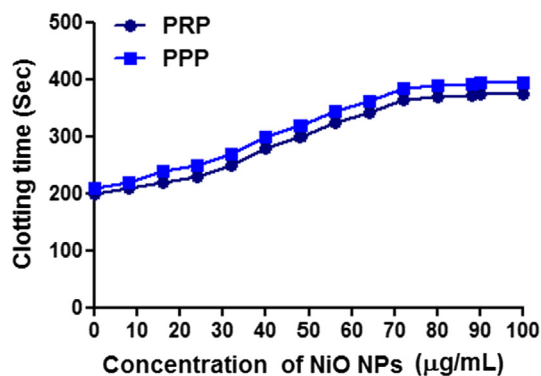


Fig. 6 Show the plasma re-calcification time was performed using both human platelet rich plasma (PRP) and platelet poor plasma (PPP) of biosynthesized NiO NPs.

death. As a results indicates that, the biosynthesized NiO NPs as size as size is very less, stability is high conveyed with large surface area to volume ratio, it simplifies that, the cell was interaction and increased the bactericidal activity with releases of Ni²⁺ ions released, easily penetrate to the cell wall and then later disturb the electron transport system and affect the com-

ponents of cells, protein, DNA and oxidative stress was induced, which finally cell was damaged. The subsequently, the bactericidal activity and stability of NiO nanoparticles are high effective, they could be employed in as antimicrobial coatings that will be helpful for various environmental and biomedical applications (Nagajyothi et al., 2014).

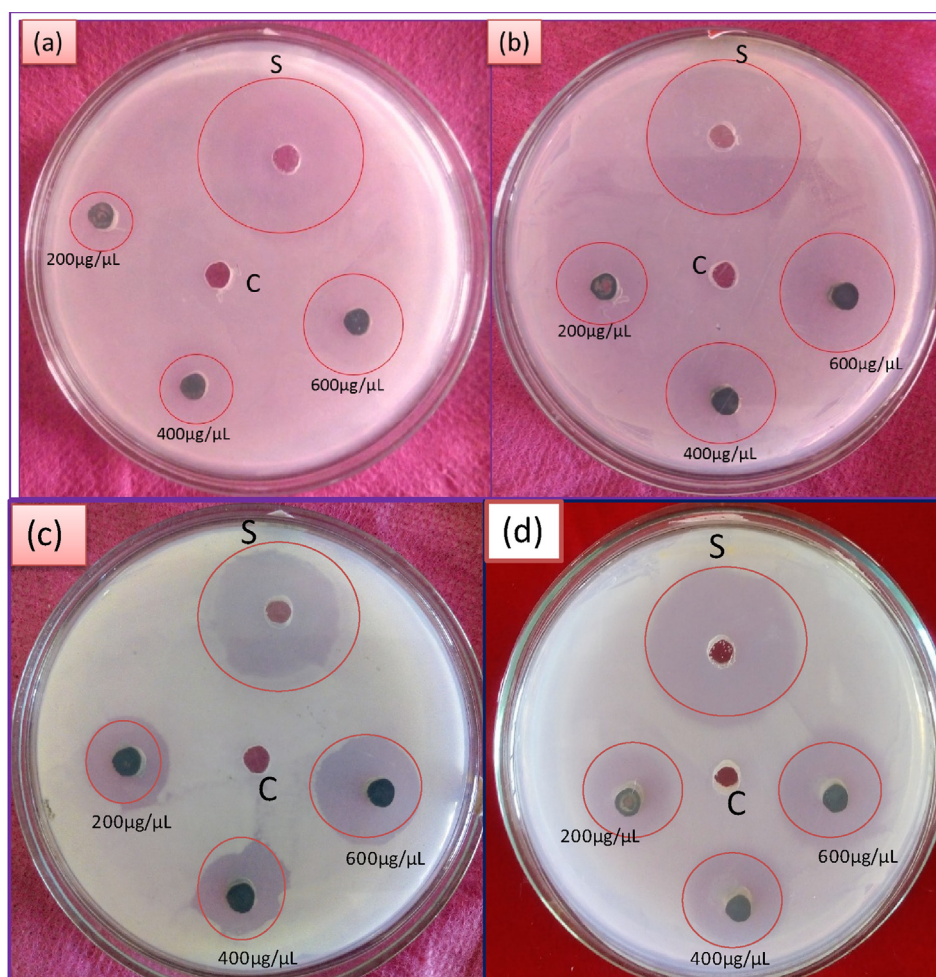


Fig. 7 The antibacterial activity of biosynthesized NiO NPs against pathogenic bacterial strains (a) *S.aureus* (b) *E.coli* (c) *Pseudomonas desmolyticum* and (d) *Klebsiella aerogenes*.

Table 1 Antibacterial activity of NiO NPs against pathogenic bacterial strains.

Treatment		Bacterial strains			
Sample	Concentration (µg/mL)	<i>S. aureus</i> (Mean ± SE)	<i>E. coli</i> (Mean ± SE)	<i>P. desmolyticum</i> (Mean ± SE)	<i>K. aerogenes</i> (Mean ± SE)
Ciprofloxacin	10	14.08 ± 0.22	11.43 ± 0.23	11.50 ± 0.29	12.02 ± 0.13
NiO NPs	200	2.43 ± 0.15	3.17 ± 0.17	3.23 ± 0.15	3.43 ± 0.12
	400	4.23 ± 0.15	5.27 ± 0.15	5.30 ± 0.06	5.33 ± 0.09
	600	8.23 ± 0.15	9.23 ± 0.15	7.33 ± 0.09	7.10 ± 0.21

Values are the mean ± SE of inhibition zone in mm.

3.2.3. Cytotoxicity activity

The evaluation of cytotoxicity of biosynthesized NiO NPs against A549 and HepG2 cell line cancer cells were measured on cellular reduction of MTT based on *invitro* analysis. The treated with NiO NPs was screened against cell lines with respective positive control as Cisplatin and control as shown in the Fig. 8. As a result shown that, the viability assay of cytotoxicity of NiO NPs against cancer cell line as shown in the Table 2. The decrease of cell viability with increasing the concentration of NiO NPs as shown significant cytotoxicity to

accumulate the internal cells and higher stress, ultimately leading to apoptosis (Song et al., 2012).

4. Conclusion

In conclusion, NiO Nanoparticles (NiO NPs) was successfully prepared via biosynthesis route using aqueous leaves extract of *E. heterophylla* [L.] leaf extract act as reducing/capping/stabilizing agent for the first time. Formation of NiO NPs was confirmed by analytical techniques such as XRD, UV-Vis, FT-IR,

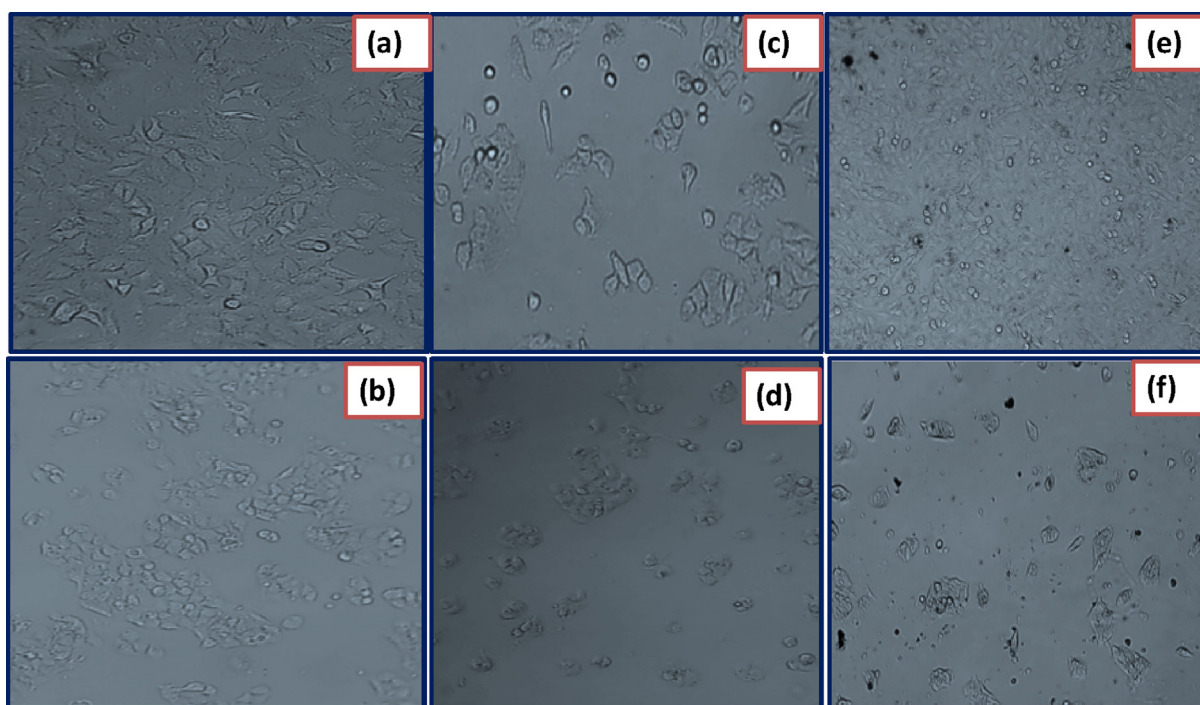


Fig. 8 Photographs on cytotoxicity studies against cancer cell lines such as A549 (a) HepG2 (b) control-cell untreated. A549 (c) HepG2 (d) cell lines treated with standard drug Cisplatin and A549 (e) HepG2 (f) Cells treated with biosynthesized NiO NPs.

Table 2 Cytotoxicity of biosynthesized NiO NPs against cancer cell lines.

Cell lines	Standard (Cisplatin) (25 μ M)	Control	NiO NPs (μ g/mL)					IC ₅₀ (μ g/mL)
			25	50	100	200	400	
A549	49.09 \pm 0.002	100 \pm 0.00	93.15 \pm 0.005	84.15 \pm 0.002	78.95 \pm 0.003	67.17 \pm 0.003	45.16 \pm 0.003	353.161
HepG2	54.48 \pm 0.00	100 \pm 0.00	95.205 \pm 0.001	84.31 \pm 0.002	70.97 \pm 0.001	58.48 \pm 0.002	47.23 \pm 0.005	344.26

SEM-EDAX and TEM. Further, the application of Direct haemolytic and Anticoagulant properties, antibacterial and cytotoxicity of biosynthesized NiO NPs consists of nano holes with various pore size was confirmed. As results show that, biosynthesized NiO nanoparticles are biocompatible material for finding the various applications.

Declaration of Competing Interest

All the authors states that there is no conflict of interest regarding this manuscript to publish in your reputed journal.

Acknowledgement

The authors express sincere thanks to Tumkur University, Tumkur, for providing the lab facilities to carry out a part of this work.

References

Ardlie, N.G., Han, P., 1974. Enzymatic basis for platelet aggregation and release: the significance of the 'platelet atmosphere' and the

relationship between platelet function and blood coagulation. *J. Haematol* 26, 331–356.

Chethana, R., Sharath Kumar, M.N., Jayanna, K., Ashwini, S., Chandramma, , Girish, K.S., Kemparaju, K., Devaraja, S., 2017. Evaluation of anticoagulant and antiplatelet activity of *Pisum sativum* pod extract. *J. Blood Res Hematol Dis.* 2 (1), 1–8.

Dhaneswar, D., Chandra Nath, B., Phukon, P., Kalita, A., Kumar Dolui, S., 2013. Synthesis of NiO nanoparticles and evaluation of antioxidant and cytotoxic activity. *Colloid Surf. B: Biointer.* 11 (1), 556–560.

Ezhilarasi, A.A., Vijaya, J.J., Kaviyarasu, K., Kennedy, J., Ramalingam, R.J., Al- Lohedan, H.A., 2018. Green synthesis of NiO nanoparticles using *Aegle marmelos* leaf extract for the evaluation of in-vitro cytotoxicity, antibacterial and photocatalytic properties. *J. Photochem. Photobiol. B Biol.* 180, 39–50.

Ezhilarasi, A.A., Vijaya, J.J., Kaviyarasu, K., Maaza, M., Aye-shamariam, A., Kennedy, L.J., 2016. Green synthesis of NiO nanoparticles using *Moringa Oleifera* extract and their biomedical applications: cytotoxicity effect of nanoparticles against HT-29cancer cells. *J. Photochem. Photobiol. B Biol.* 164, 352–360.

Falodun, A., Agbakwuru, E.O.P., 2004. Phyto-chemical analysis and laxative activity of the leaf extracts of *Euphorbia heterophylla* L. (Euphorbiaceae). *Pak. J. Sci. Ind. Res.* 47 (5), 345–348.

Falodun, A., Okunrobo, L.O., Uzoamaka, N., 2006. Phytochemical screening and anti-inflammatory evaluation of methanolic and

- aqueous extracts of *Euphorbia heterophylla* Linn (Euphorbiaceae). African J. Biotechnol. 5 (6), 529–531.
- Gnanasekaran, L., Hemamalini, R., Saravanan, R., Ravichandran, K., Gracia, F., Agarwal, S., Gupta, V.K., 2017. Synthesis and characterization of metal oxides (CeO₂, CuO, NiO, Mn₃O₄, SnO₂ and ZnO) nanoparticles as photo catalysts for degradation of textile dyes. J. Photochem. Photobiol. B 173, 43–49.
- Hisatomi, T., Kubota, J., Domen, K., 2014. Recent advances in semiconductors for photocatalytic and photo electro chemical water splitting. Chem. Soc. Rev. 43, 7520–7535.
- Hoffmann, M.R., Martin, S.T., Choi, W., Bahnemann, D.W., 1995. Environmental applications of semiconductor photocatalysis. Chem. Rev. 95, 69–96.
- Ibraheem, F., Aziz, M.H., Fatima, M., Shaheen, F., Mansoor Ali, S., Huang, Q., 2019. *In vitro* cytotoxicity, MMP and ROS activity of green synthesized nickel oxide nanoparticles using extract of *Terminalia chebula* against MCF-7 cells. Mater. Lett. 234 (1), 129–133.
- Jahromi, S.P., Pandikumar, A., Goh, B.T., Lim, Y.S., Basirun, W.J., Lim, H.N., Huang, N.M., 2015. Influence of particle size on performance of a nickel oxide nanoparticle-based supercapacitor. RSC Adv. 5 (18), 14010–14019.
- Kaviyarasu, K., Manikandan, E., Kennedy, J., Jayachandran, M., Lachumananandasiivam, R., Umbelino De Gomes, U., Maaza, M., 2016. Synthesis and characterization studies of NiO Nano rods for enhancing solar cell efficiency using photonupconversion materials. Ceram. Int. 42, 8385–8394.
- Keerthana, K., Deepa, A., Shobana, G., Jothi, G., Sridharan, G., 2014. Preliminary phytochemical screening and *invitro* antioxidant potential of *Euphorbia heterophylla* (L.). Inter. J. Pharm. Pharm. Sci. 6 (8), (15).
- Lingaraju, K., Raja Naika, H., Nagabhushana, H., Nagaraju, G., 2019. *Euphorbia heterophylla* (L.) mediated fabrication of ZnO NPs: Characterization and evaluation of antibacterial and anticancer properties. Biocatal. Agri. Biotech. 18, 100894.
- Madhumitha, G., Elango, G., Roopan, S.M., 2016. Biotechnological aspects of ZnO nanoparticles: overview on synthesis and its applications. Appl. Microbiol. Biotechnol. 100 (2), 571–581.
- Manivel, P., Roopan, S.M., Kumar, R.S., Khan, F.N., 2009. Synthesis of 3 substituted isoquinolin-1-yl-2-(cycloalk-2-enylidene) hydrazines and their antimicrobial properties. J. Chil. Chem. Soc. 54, 183–185.
- Manjunath, K., Ravishankar, T.N., Kumar, Dhanith, Priyanka, K.P., Varghese, Thomas, Raja Naika, H., Nagabhushana, H., Sharma, S.C., Dupont, J., Ramakrishnappa, T., Nagaraju, G., 2014. Facile combustion synthesis of ZnO nanoparticles using *Cajanuscajan* (L.) and its multidisciplinary applications. Mater. Res. Bull. 7, 325–334.
- Meenakshi Sundaram, M., Karthikeyan, K., Sudarsanam, D., Brindha, P., 2010. Antimicrobial and anticancer studies on *Euphorbia heterophylla*. J. Pharm. Res. 3 (9), 2332–2333.
- Mohammadijoo, M., Khorshidi, Z.N., Sadrnezhaad, S.K., Mazinani, V., 2014. Synthesis and characterization of nickel oxide nanoparticle with wide band gap energy prepared via thermochemical processing. Nano Sci. Nanotechnol.: Int. J. 4, 6–9.
- Motevalli, K., Zarghami, Z., Panahi-Kalamuei, M., 2016. Simple, novel and low-temperature synthesis of rod-Like NiO nanostructure via thermal decomposition route using anew starting reagent and its photocatalytic activity assessment. J. Mater. Sci. Mater. Electron. 27, 4794–4799.
- Nagajyothi, P.C., Sreekanth, T.V.M., Clement, O., Tettey, Jun, Y.I., Heung, , Mook, S., 2014. Characterization antibacterial, antioxidant, and cytotoxic activities of ZnO nanoparticles using *Coptidis Rhizoma*. Bio. Org. Med. Chem. Lett. 24 (17), 4298–4303.
- Nandy, S., Goncalves, G., Pinto, J.V., Busani, T., Figueredo, V., Pereira, L., Martins, R.F.P., Fortunato, E., 2013. Current transport mechanism at metal-semiconductor nanoscale interfaces based on ultrahigh density arrays of p-type NiO nano-pillars. Nanosca. 5, 11699–11709.
- Nassar, M.Y., Aly, H.M., Abdelrahman, E.A., Moustafa, M.E., 2017. Synthesis, characterization and biological activity of some novel Schiff bases and their Co(II) and Ni(II)complexes: a new route for Co₃O₄ and NiO nanoparticles for photocatalytic degradation of methylene blue dye. J. Mol. Struct. 1143, 462–471.
- Nasseri, M.A., Ahrari, F., Zakerinasab, B.A., 2016. Green Biosynthesis of NiO nanoparticles using aqueous extract of *Tamarix serotina* and their characterization and application. Appl. Organomet. Chem. 30, 978–984.
- Pereira, S., Gonçalves, A., Correia, N., Pinto, J., Pereira, L.Í., Martins, R., Fortunato, 2014. Electro chromic behavior of NiO thin films deposited by e-beam evaporation at room temperature. Sol. Energy Mater. Sol. Cell 120, 109–115.
- Qing, Z., Haixia, L., Huali, L., Yu, L., Huayong, Z., Tianduo, L., 2015. Solvothermal synthesis and photocatalytic properties of NiO ultrathin nanosheets with porous structure. Appl. Surf. Sci. 328, 525–530.
- Quick, A.J., Stanley-Brown, M., Bancroft, F.W., 1935. A study of the coagulation defect in hemophilia and in jaundice. Am. J. Med. Sci. 190, 501–511.
- Raja Naika, H., Krishna, V., 2006. Antimicrobial activity of extracts from the leaves of *Clematis gouriana* Roxb. Inter. J. Biomed. Pharma. Sci. 1, 69–72.
- Rajesh Kumar, A.S., Kishore, N., Budhiraja, N., 2013. Preparation and characterization of NiO nanoparticles by co-precipitation method. Inter. J. Eng. Appl. Manag. Sci. Para. 06, 64–67.
- Roopan, S.M., Khan, F.R.N., 2011. SnO₂ nanoparticles mediated non-traditional synthesis of biologically active 9-chloro-6,13-dihydro-7-phenyl-5H-indolo [3,2-c]- acridine derivatives. Med. Chem. Res. 20, 732–737.
- Sankar, S., Sharma, S.K., An, N., Lee, H., Kima, D.Y., Im, Y.B., Cho, Y.D., Ganesh, R.S., Ponnusamy, S., Raji, P., Purohit, L.P., 2016. Photocatalytic properties of Mn-doped NiO spherical nanoparticles synthesized from sol-gel method. Optik Int. J. Light Electron. Opt. 127, 10727–10734.
- Singh, P., Kim, Y.J., Zhang, D., Yang, D.C., 2016. Biological synthesis of nanoparticles from plants and microorganisms. Trends Biotechnol. 34 (7), 588–599.
- Sone, B.T., Fuku, X.G., Maaza, M., 2016. Physical & electrochemical properties of green synthesized bunsenite NiO nanoparticles via *Callistemon viminalis* extracts. Int. J. Electrochem. Sci. 11, 8204–8220.
- Sun, C., Liab, H., Chen, L., 2012. Nanostructured ceria-based materials: synthesis, properties, and applications. Energy Environ. Sci. 5, 8475–8505.
- Suresh, D., Nethravathi, P.C., Rajanaika, H., Nagabhushana, H., Sharma, S.C., 2015. Green synthesis of multifunctional zinc oxide (ZnO) nanoparticles using *Cassia fistula* plant extract and their photodegradative, antioxidant and antibacterial activities. Mater. Sci. Semicond. Process 31, 446-454.
- Thema, F.T., Manikandan, E., Gurib-Fakim, A., Maaza, M., 2016. Single phase bunsenite NiO nanoparticles green synthesis by *Agathosma betulina* natural extract. J. Alloy. Comp. 657, 655–661.
- Uduak, A., Essiet, K., Ajibesin, K., 2010. Antimicrobial activities of some euphorbiaceae plants used in the traditional medicine of Akwa Ibom state of Nigeria. Ethnobotanical Leaflets 14, 654–664.
- Zhi-Guo, Y., Li-Ping, Z., Yan-Min, G., Zhi-Zhen, Y., Bing-Hui, Z., 2011. Preparation and band-gap modulation in Mg_xNi_{1-x}O thin films as a function of Mg contents. Thin Solid Films 519, 5174–5177.